A monolithic 20GHz integrated extended cavity mode-locked quantum well ring laser at 1.58μm fabricated in the JEPPIX platform

A Monolithic 20GHz Integrated Extended Cavity Mode-locked Quantum Well Ring Laser at 1.58µm Fabricated in the JEPPIX Platform

M.S. Tahvili*, Y. Barbarin†, X.J.M. Leijtens, T. de Vries, E. Smalbrugge, J. Bolk, H.P.M.M. Ambrosius, M.K. Smit, and E.A.J.M. Bente
COBRA Research Institute, Technical University of Eindhoven, Eindhoven, the Netherlands

We report on a passively modelocked InP/InGaAsP quantum well semiconductor ring laser which operates at 20GHz repetition rate and at 1.58µm output wavelength. A number of devices with varying relative positions of the absorbers and amplifiers have been realized using active-passive integration technology in the JEPPIX fabrication platform. The 4mm-long laser ring cavity incorporates a 750µm-long optical amplifier section, a separate 40µm-long saturable absorber section, passive waveguide sections and a passive MMI-type 50% output coupler. We investigate operation regimes of the laser and explore conditions for single mode lasing and mode-locked operation.

Introduction

Semiconductor mode-locked lasers are of particular interest for generation of stable optical pulses in different fields of optical communication and also novel applications such as all-optical sampling [1]. Ring cavities offer important advantages over Fabry-Pérot type structures. The cavity length and hence the repetition rate of a mode-locked ring laser is designed and determined accurately by lithography during fabrication as opposed to a device with cleaved facet mirrors. More importantly, a ring laser can be located freely on a photonic integrated circuit, and be directly integrated with other optical components on an optical chip.

In this paper, we present mode-locked operation of a monolithic 20GHz integrated extended cavity ring laser. The 4mm-long laser ring cavity incorporates a 750µm-long optical amplifier section (SOA-section), a separate 40µm-long saturable absorber (SA) section, passive waveguide sections (shallow and deep etch) and a passive MMI-type 50% output coupler. The active sections contain a four quantum well active layer. The output waveguides are tilted under an angle of 7° to minimize back reflections into the device. Fig.1 shows a top view of the ring laser under microscope. Fabrication of a number of devices with varying relative positions of the absorbers and amplifiers has been carried out in the JEPPIX platform [2].

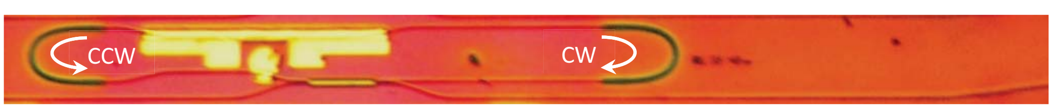

Fig.1. Top view of the ring laser under test. The optical amplifier and absorber sections are seen as a large metalized pad and a small circular contact pad respectively. Shallow and deep etched passive waveguides are visible as thin dark lines and thick bends respectively. The left output arm is not shown completely.

*Correspondence: s.tahvili@tue.nl
†Yohan Barbarin is currently with the Institute for Quantum Electronics, Swiss Federal Institute of Technology (ETH) Zurich, Switzerland.

In principle, a ring structure supports two counter propagating fields. In mode-locked regime, clockwise (CW) and counter clock-wise (CCW) propagating pulses in the ring laser cavity will meet in the SA-section to saturate the absorber. In the current device layout, the relative position of SOA and SA sections in the cavity is designed such that the counter propagating pulses will also meet just at the right hand side of the gain section (see Fig.1). This means that the CCW-propagating pulse will enter the SOA-section just after the amplifier gain is depleted by the CW pulse. Therefore, the asymmetrical design of the device under test could lead to (quasi-)unidirectional performance of the laser in favor of the CW propagating pulses [3].

Experimental Results

The chip is mounted on a copper chuck which is temperature stabilized at 12^{o}C using a thermistor and Peltier element which in turn is water cooled. The output light from the devices is collected by two lensed fibers with anti-reflection coated tips at the left and right facets of the chip. The device is operated by current injection to the SOA-section (I_{SOA}) and reverse-biasing the SA-section (V_{SA}).

In order to map the region of mode-locking (ML) in terms of operating parameters, i.e. I_{SOA} and V_{SA}, we could observe the RF spectra recorded by a 50GHz electrical spectrum analyzer (ESA) connected to a fast photodiode. The height of RF peak at fundamental frequency (repetition rate) can then be used as an indication of the quality of mode-locking. In Fig.2 the height of RF peaks at fundamental frequency over the noise floor of the ESA (presented by circles) and also over other low frequency components of the spectrum (presented by squares) is color coded in a dB scale. Two different regimes of ML operation are observed in Fig.2. The first region is for bias values of V_{SA}=–2.2V to –2.7V where the laser shows ML operation for a range of I_{SOA} which is indicated in the figure. At V_{SA}=–2.8V the locked state is no longer observed and the laser remains in continuous wave mode as I_{SOA} is increased above threshold. However, if we start to reduce the current below approximately 100mA, the device will enter an ML state as a result of a hysteresis-like effect. We will not discuss this situation further in this paper and therefore it is not included on the ML map. A second regime of ML is observed for V_{SA}=–3V to –3.6V, where I_{SOA} varies in the range of 110mA to 150mA. In this regime, the transition from continuous wave operation to locked state seems more instantaneous than in the first regime as the current is increased.

To study characteristics of ML in the two regimes mentioned, we consider one operating point associated with each regime. The two operating points are I_{SOA}=55mA at V_{SA}=–2.6V, point P1, and I_{SOA}=120mA at V_{SA}=–3.2V, point P2. Fig. 3 shows fiber coupled output power of the CW and CCW fields at operating points P1 and P2. The threshold current increases from 24mA to 33mA for values of V_{SA}=0V down to –3.2V. At V_{SA}=–2.6V the power of CW and CCW fields measured at left and right output arms are approximately the same up to 43mA (onset of ML region). Increasing I_{SOA} above the onset of ML, induces a change in the ratio of CW and CCW output power levels. At operating point P1 the ratio of fiber-coupled output power of CW propagating to the

CCW pulses is ~3.5dB. In the locked state at V_{SA}=–3.2V, a clear change in CW and CCW output power levels is observed. The maximum achieved directionality ratio (CW/CCW) in this case is ~5.5dB at I_{SOA}=128mA.

At operating point P1, the 50GHz RF spectrum trace demonstrates clear RF peaks at f_{rep}=19.627GHz and the second order harmonic. The peak at fundamental frequency is more than 40dB over noise floor with full width at half maximum (FWHM) of 200kHz. The width at -20dB below the top of the peak is ~1MHz. The value of timing jitter is determined to be 7.9ps. This value is calculated by integration of single sideband phase noise signal over 10kHz-80MHz offset around the fundamental frequency. The RF spectrum for the device operating at point P2 shows repetition rate of f_{rep}=19.622GHz. The peak is at least 38dB higher than other frequency components in the spectrum and has FWHM of 500kHz. The width at -20dB below the top of the peak in this case is 4.2MHz. Furthermore, the value of timing jitter is calculated to be 10.8ps.

To confirm pulsed operation of the device, autocorrelator (AC) traces of the output optical signal (CW) have been recorded. Background free AC indicates a FWHM (Gaussian fit) of approximately 4.78ps and 3.58ps for operating points P1 and P2 respectively. The AC traces are given in Fig.4.

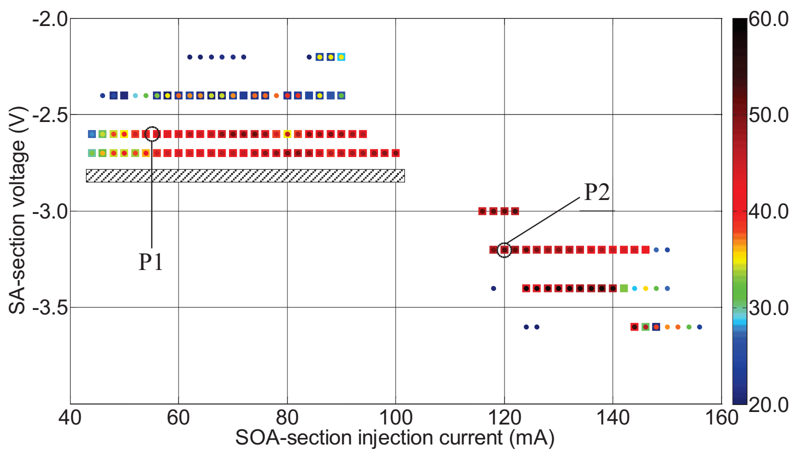

Fig.2. Height of RF peak (color-coded in dB scale) at fundamental frequency over the noise floor (circles) of the electrical spectrum analyzer, and over all the lower frequency components (squares). Operating points P1 (I_{SOA}=55mA, V_{SA}=–2.6V) and P2 (I_{SOA}=120mA, V_{SA}=–3.2V) are indicated on the figure. The ML regime at V_{SA}=–2.8 (hashed area) is not discussed in this paper.

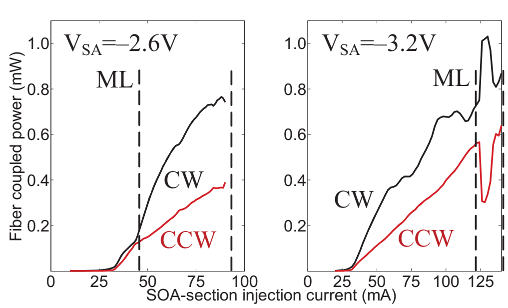

Fig.3. Fiber coupled output power of the ring mode-locked laser (CW in black and CCW in red) as a function of SOA-section injection current.

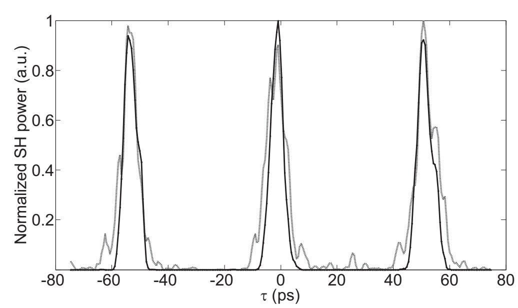

Fig.4. Autocorrelator traces of the CW optical pulses at I_{SOA}=55mA, V_{SA}=–2.6V (dashed grey) and I_{SOA}=120mA, V_{SA}=–3.2V (solid black).

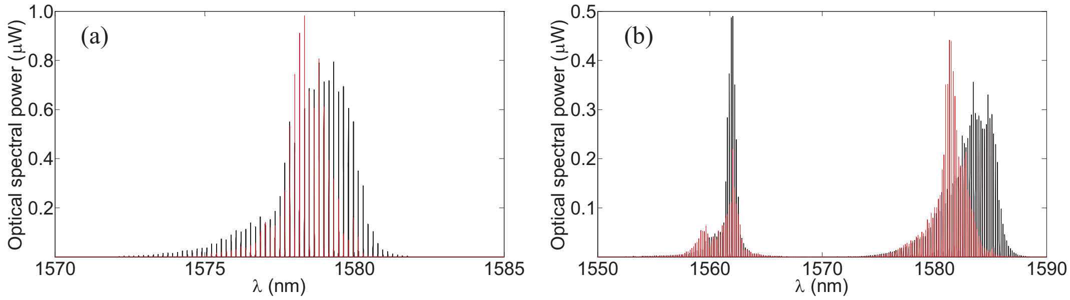

Fig.5. High resolution (0.16pm) optical spectrum (linear scale) of the output light CW (black) and right CCW(red) at operating points (a) P1 and (b) P2.

The major difference between two ML regimes is the shape of the optical spectrum. At V_{SA}=–2.6V the device operates as a continuous wave single mode laser around 1576nm for I_{SOA}=35mA to 43mA. Increasing the current further will derive the device to the ML region and shifts the spectrum to wavelengths around 1579nm. The optical spectra of the CW and CCW propagating pulses at point P1 are shown in Fig.5(a). At V_{SA}=–3.2V the device operates like a multimode laser in the wavelength range 1550-1560nm and for injection currents up to around 118mA. At the onset of ML a second group of modes emerge around 1580nm and the optical spectrum changes shape. The optical spectra of counter propagating pulses at point P2 is shown in Fig.5(b). The difference in shape and wavelength of CW and CCW optical spectra is more emphasized in this case.

Conclusions

Two mode-locked operation regimes of a monolithic 20GHz integrated extended cavity ring laser have been studied. Directional operation of the ring laser in favor of the CW propagating pulses is shown to be predicted correctly by our simulation model. The power ratio observed between the counter propagating pulses (CW/CCW) in mode-locked state is 2.5-5.5dB, which is however, lower than the expected value for the asymmetric design. Optical pulses with a stable repetition rate and duration in the order of ps are achieved. The value of timing jitter is in the range of 7-10ps. The optical spectra of counter propagating pulses show significant differences.

Acknowledgements

Authors acknowledge the JEPPIX technology platform for provision of devices. This work is supported by IOP Photonic Devices program managed by the Technology Foundation STW and Agentschap NL.

References

[1] S. Cheung, et. al., "Super-Long Cavity, Monolithically Integrated 1-GHz Hybrid Mode-Locked InP Laser for All-Optical Sampling," in Photonics in Switching, OSA Technical Digest (CD) (Optical Society of America, 2010), paper PWD2.

[2] For more information about JEPPIX platform: www.jeppix.eu.

[3] E.A.J.M. Bente, et. al., "Modeling of integrated extended cavity InP/InGaAsP semiconductor modelocked ring lasers," Opt. and Quantum Electron., vol. 40, pp. 131-148, 2008.